J|A|C|S
ARTICLES
Published on Web 03/21/2003

# Doping-Controlled Ion Diffusion in Polyelectrolyte Multilayers: Mass Transport in Reluctant Exchangers

Tarek R. Farhat† and Joseph B. Schlenoff*

*Contribution from the Department of Chemistry and Biochemistry and Center for Materials Research and Technology (MARTECH), The Florida State University, Tallahassee, Florida 32306*

Received December 16, 2002; E-mail: schlen@chem.fsu.edu

***Abstract:*** A new paradigm for nonlinear doping-controlled ion transport in soft condensed matter is presented, where the mobility of a minority "probe" ion is controlled by majority "salt" ion. The class of materials to which this paradigm applies is represented by ultrathin films of polyelectrolyte complexes, or multilayers. Intersite hopping of probe ions of charge $\nu$ occurs only when the charge of the destination site, produced by clustering of monovalent salt ions, is at least $-\nu$, conserving electroneutrality. Salt ions are reversibly "doped" into the multilayer under the influence of external salt concentration. In situ ATR-FTIR reveals that the doping level, $y$, is proportional to salt concentration. Because hopping requires coincidence, or clustering, of salt, a strongly nonlinear dependence of flux, $J$, on salt concentration is observed: $J \sim [\mathrm{NaCl}]^{\nu} \sim y^{\nu}$. This scaling was reproduced both by Monte Carlo simulations of ion hopping and by continuum probability expressions. The theory also predicts the observed scaling, though it underestimates the magnitude, of the strong selectivity of multilayers for ions of different charge.

## Introduction

Ultrathin films of polyelectrolyte complexes may be deposited on substrates by exposing them, in an alternating fashion, to solutions of oppositely charged polymers.[1] These "polyelectrolyte multilayers" (PEMUs) are generally amorphous[1a,d,2,3] due to extensive interpenetration of polymer molecules driven by efficient ion pairing between complementary charged polyelectrolyte segments, a property that tends to exclude small counterions from the bulk.[4,5] Excess polymer charge, required for the layer-by-layer growth of PEMUs, resides at the surface, is balanced by salt counterions, and is diffused over a thickness of a few nominal "layers".[4,6,7] PEMUs have shown exceptional promise as selective membranes for the controlled transport[8] and release[9] of small molecules and for the immobilization of (bio)macromolecules[10] or particles.[11]

Using electrodes coated with PEMUs, it was found that salt added to the external solution controlled the permeation of other, electrochemically active, charged species. Transport was faster for species of lower charge, and the flux through the multilayer, as well as the selectivity, was controlled by the solution salt concentration.[12] Although PEMUs contain no bulk salt counterions in their nascent state,[4,5] the chemical potential of solution salt contacting the multilayer generates sites for small ion exchange within the PEMU. The term "reluctant exchanger" was used to describe a material that requires such conditions to force the creation of ion exchange sites.[12] Observation of the reversible swelling of a PEMU as salt ions are introduced permitted a comparison of the relative formation energies of

† Current address: Department of Chemical Engineering, Massachusetts Institute of Technology, Cambridge, MA 02139.

(1) (a) Decher, G., Schlenoff, J. B., Eds. *Multilayer Thin Films−Sequential Assembly of Nanocomposite Materials*; Wiley-VCH: Weinheim, 2002. (b) Decher, G. *Science* **1997**, *277*, 1232. (c) Decher, G. In *Comprehensive Supramolecular Chemistry*; Sauvage, J. P., Hosseini, M. W., Eds.; Pergamon Press: Oxford, 1996; Vol. 9, Chapter 14. (d) Bertrand, P.; Jonas, A.; Laschewsky, A.; Legras, R. *Macromol. Rapid Commun.* **2000**, *21*, 319.
(2) (a) Schmitt, J.; Grünewald, T.; Decher, G.; Pershan, P. S.; Kjaer, K.; Lösche, M. *Macromolecules* **1993**, *26*, 7058. (b) Lösche, M.; Schmitt, J.; Decher, G.; Bouwman, W. G.; Kjaer, K. *Macromolecules* **1998**, *31*, 8893.
(3) Farhat, T.; Yassin, G.; Dubas, S. T.; Schlenoff, J. B. *Langmuir* **1999**, *15*, 6621.
(4) Schlenoff, J. B.; Ly, H.; Li, M. *J. Am. Chem. Soc.* **1998**, *120*, 7626.
(5) Bixler, H. J.; Michaels, A. *Encylcopedia of Polymer Science and Technology*; Interscience: New York, 1969; Vol. 10, p 765.
(6) Dubas, S. T.; Schlenoff, J. B. *Macromolecules* **1999**, *32*, 8153.
(7) Schlenoff, J. B.; Dubas, S. T. *Macromolecules* **2001**, *34*, 592.
(8) (a) Stroeve, P.; Vasquez, V.; Coelho, M. A. N.; Rabolt, J. F. *Thin Solid Films* **1996**, *284*, 708. (b) Levasalmi, J.; McCarthy, T. J. *Macromolecules* **1997**, *30*, 1752. (c) Harris, J. J.; Bruening, M. L. *Langmuir* **2000**, *16*, 2006. (d) Krasemann, L.; Tieke, B. *Langmuir* **2000**, *16*, 287. (e) Harris, J. J.; DeRose, P. M.; Bruening, M. L. *J. Am. Chem. Soc.* **1999**, *121*, 1978. (f) Dai, J.; Balachandra, A. M.; Lee, J. I.; Bruening, M. L. *Macromolecules* **2002**, *35*, 3165. (g) Balchandra, A. M.; Dai, J.; Bruening, M. L. *Macromolecules* **2001**, *35*, 3171. (h) Dai, J.; Jensen, A. W.; Mohanty, D. K.; Erndt, J.; Bruening, M. L. *Langmuir* **2001**, *17*, 931. (i) Krasemann, L.; Tieke, B. *J. Membr. Sci.* **1998**, *150*, 23. (j) Van Ackern, F.; Krasemann, L.; Tieke, B. *Thin Solid Films* **1998**, *327−329*, 762. (k) Krasemann, L.; Toutianoush, A.; Tieke, B. *J. Membr. Sci.* **2001**, *181*, 221. (l) Toutianoush, A.; Tieke, B. In *Novel Methods to Study Interfacial Layers*; Möbius, D., Miller, R., Eds.; Elsevier: New York, 2001.
(9) (a) Caruso, F.; Donath, E.; Mohwald, H. *J. Phys. Chem. B* **1998**, *102*, 2011. (b) Donath, E.; Sukhorukov, G. B.; Caruso, F.; Davis, S. A.; Mohwald, H. *Angew. Chem., Int. Ed. Engl.* **1998**, *37*, 2202. (c) Caruso, F.; Lichtenfeld, H.; Giersig, M.; Mohwald, H. *J. Am. Chem. Soc.* **1998**, *120*, 8523. (d) Caruso, F.; Caruso, R. A.; Mohwald, H. *Science* **1998**, *282*, 1111. (e) Chung, A. J.; Rubner, M. F. *Langmuir* **2002**, *18*, 1176.
(10) (a) Decher, G.; Lehr, B.; Lowack, K.; Lvov, Y.; Schmitt, J. *Biosens. Bioelectron.* **1994**, *9*, 677. (b) Sun, Y.; Zhang, X.; Sun, C.; Wang, B.; Shen, J. *Macromol. Chem. Phys.* **1996**, *197*, 147. (c) Onda, M.; Lvov, Y.; Ariga, K.; Kunitake, T. *Biotechnol. Bioeng.* **1996**, *51*, 163. (d) Lvov, Y. M.; Lu, Z.; Schenkman, J. B.; Rusling, J. F. *J. Am. Chem. Soc.* **1998**, *120*, 4073.
(11) (a) Iler, R. K. *J. Colloid Interface Sci.* **1966**, *21*, 569. (b) Kleinfeld, E. R.; Ferguson, G. S. *Science* **1994**, *265*, 370. (c) Watanabe, S.; Regan, S. L. *J. Am. Chem. Soc.* **1994**, *116*, 8855. (d) Feldheim, D. L.; Grabar, K. C.; Natan, M. J.; Mallouk, T. C. *J. Am. Chem. Soc.* **1996**, *118*, 7640. (e) Lvov, Y.; Ariga, K.; Onda, M.; Ichinose, I.; Kunitake, T. *Langmuir* **1997**, *13*, 6195. (f) Kotov, N. A.; Dekany, I.; Fendler, J. H. *J. Phys. Chem.* **1995**, *99*, 13065.
(12) Farhat, T. R.; Schlenoff, J. B. *Langmuir* **2001**, *17*, 1184.

pairs of polyelectrolytes.[13] If one of the polyelectrolytes is a weak acid, protonation and salt content of the multilayer are coupled, and the salt concentration controls the effective p$K_a$ of the weak polyacid/polybase.[14]

The lack of compositional modulation,[2] or actual "multilayering", in PEMUs confers valuable simplicity on the analysis, reducing the system to one that responds homogeneously to a few equilibrium constants. We apply these key equilibria without recourse to complex electrostatic arguments and the usual high-salt-concentration dilemmas[15] they entail.

Small counterions and charged polymer segments participate within a PEMU to maintain net charge neutrality. A polymer segment, Pol, paired with another, oppositely charged, segment is "intrinsically" compensated, whereas Pol neutralized by a salt counterion represents "extrinsic" compensation. A system having predominantly persistent extrinsic charge will behave as a classical fixed-site "Donnan" ion exchanger, excluding species of the same charge as the fixed site and including those of opposite charge.[16] We have discussed strategies for introducing extrinsic charge into multilayered systems,[4,7,17] and there are currently attempts to control this parameter and the enhanced selectivity it may offer.[8f−h]

The introduction of exchange sites, by salt swelling, facilitating small ion transport, may be considered a form of doping. The utility of doping is well established, as applied to the description of electron transport in many forms of condensed matter, including "hard" materials, such as semiconductors[18] and superconductors,[19] and "soft" materials, such as conjugated polymers[20] and redox polymers.[21] In these cases, doping produces a carrier and the mobile species are electrons. In the present work, we coordinate experimental and theoretical evaluations of reversible physical doping of reluctant exchangers and the transport of multiply charged species. In doing so we verify, experimentally, two of the essential elements underpinning the concept of reluctant exchange. The results have far-reaching implications for the reversible control of membrane transport.

## Background

Using simple equilibrium arguments, it may be shown that an intrinsic PEMU may be converted to one that bears extrinsic sites by exposure to a solution containing salt.[12] The system essentially behaves as a variable capacity ion exchanger. For example,

$$Pol^+Pol^-_{(m)} + Cl^-_{(aq)} + Na^+_{(aq)} \rightleftharpoons Pol^+Cl^-_{(m)} + Pol^-Na^+_{(m)} \quad (1)$$

Equation 1 shows how salt moderates the interaction of positive ($Pol^+$) and negative ($Pol^-$) polymer segments. $Pol^+Pol^-$ is an intrinsically compensated ion pair, and $Pol^+Cl^-$ and $Pol^-Na^+$ are extrinsic sites bearing exchangeable counterions.[22,23] A similar equation may be written for any charged species, including electrochemically active ones (i.e., capable of undergoing electron transfer at an electrode), such as ferrocyanide, used as "minority" probe ions in our membrane permeation experiments

$$4Pol^+Pol^-_{(m)} + Fe(CN)_6^{4-}{}_{(aq)} + 4Na^+_{(aq)} \rightleftharpoons Pol_4^{4+}Fe(CN)_6^{4-}{}_{(aq)} + 4Pol^-Na^+_{(m)} \quad (2)$$

The fraction of extrinsic charge, $y$, is defined as the fraction of intrinsic charge converted to extrinsic charge under the influence of added salt. For $n$ $Pol^+Pol^-$ intrinsic ion pairs, for example

$$nPol^+Pol^- + nyNa^+ + nyCl^- \rightleftharpoons (1-y)nPol^+Pol^- + nyPol^+Cl^- + nyPol^-Na^+ \quad (3)$$

Since $y$ represents the fraction of polymer charges compensated by small, mobile ions, in the context of the current work $y$ is also the "doping level".

All ions are capable of diffusing through a PEMU when it is used as a membrane.[24] Only those undergoing electron transfer, electrochemically active ions, are observed in an electrochemical experiment. Electrochemically inert ions, such as $Na^+$ and $Cl^-$, control diffusion rates but do not contribute to electrochemical current. All ions are capable of doping the multilayer via eq 3. However, under our conditions, NaCl is present in much higher concentration and thus it controls the doping level. Although both NaCl and redox probe are salts, in the context of this work, "salt" is reserved for majority counterions (usually NaCl) and "probe ion" for minority redox ion.

As ions enter the multilayer, it swells.[13] Swelling is reversible and may be represented by the appropriate equilibrium constant. For example, in pure NaCl solutions

$$K_1 = y^2/(1-y)[NaCl]_{aq}^2 \quad (4)$$

The higher the swelling constant, $K_1$, the more efficiently the PEMU is swollen, or doped, by salt. For large concentrations of "majority" salt ions compared to minority probe ions (the "high-salt" limit), doping is controlled by salt only, and is approximated by eq 4.[12] For small values of $y$, the dilute doping limit, the doping level is proportional to salt concentration (or,

(13) Dubas, S. T.; Schlenoff, J. B. *Langmuir* **2001**, *17*, 7725.
(14) Rmaile, H. H.; Schlenoff, J. B. *Langmuir* **2002**, *18*, 8263.
(15) Dautzenberg, H.; Jaeger, W.; Kötz, J.; Philipp, B.; Seidel, Ch.; Stscherbina, D. *Polyelectrolytes: Formation, Characterization and Application*; Hanser: Munich, 1994.
(16) Helfferich, F. *Ion Exchange*; McGraw-Hill: New York, 1962; Chapter 8.
(17) (a) Laurent, D.; Schlenoff, J. B. *Langmuir* **1997**, *13*, 1552. (b) Stepp, J.; Schlenoff, J. B. *J. Electrochem. Soc.* **1997**, *144*, L155.
(18) (a) Hamann, C.; Burghardt, H.; Frauenheim, T. *Electrical Conduction Mechanisms in Solids*; VEB: Berlin, 1988. (b) Lundstrom, M. *Fundamentals of Carrier Transport*, 2nd ed.; Cambridge University Press: Cambridge, U.K., 2000.
(19) Sheahen, T. P. *Introduction to High-Temperature Superconductivity*; Plenum Press: New York, 1994.
(20) Skotheim, T. A.; Elsenbaumer, R. L.; Reynolds, J. R. *Handbook of Conducting Polymers*; Marcel Dekker: New York, 1998.
(21) (a) Anson, F. C.; Saveant, J.-M.; Shigehara, K. *J. Phys. Chem.* **1983**, *87*, 214. (b) Saveant, J. M. *J. Electroanal. Chem.* **1986**, *201*, 211. (c) Murray, R. W. *Annu. Rev. Mater. Sci.* **1984**, *14*, 145. (d) Facci, J. S.; Schmehl, R. H.; Murray, R. W. *J. Am. Chem. Soc.* **1982**, *104*, 4960. (e) Surridge, N. A.; Jernigan, J. C.; Dalton, E. F.; Buck, R. P.; Watanabe, M.; Zhang, H.; Pinkerton, M.; Wooster, T. T.; Longmire, M. L.; Facci, J. S.; Murray, R. W. *Faraday Discuss. Chem. Soc.* **1989**, *88*, 1. (f) Williams, M. E.; Masui, H.; Long, J. W.; Malik, J.; Murray, R. W. *J. Am. Chem. Soc.* **1997**, *119*, 1997. (g) Wilbourn, K.; Murray, R. W. *J. Phys. Chem.* **1988**, *92*, 3642. (h) Surridge, N. A.; Sosnoff, C. S.; Schmehl, R.; Facci, J. S. Murray, R. W. *J. Phys. Chem.* **1994**, *98*, 917. (i) Jernigan, J. C.; Murray, R. W. *J. Phys. Chem.* **1987**, *91*, 2030.

(22) The strong tendency for polyelectrolyte ion pairing means that efforts to induce extrinsic charge into PEMUs have focused on postdeposition processing steps.
(23) In the salt-free limit, the "interaction energy" between polyelectrolytes is the greatest, which explains why as-made multilayers, where the last step is a rinse in pure water, contain minimal salt counterions.
(24) These doping equations do not show the waters of hydration that accompany ions as they swell the PEMU. A greater water content should enhance transport of water through the films.

more precisely, salt activity),

$$y \approx [\mathrm{NaCl}]_{aq}\sqrt{K_1} \tag{5}$$

This finding may be generalized for any salt $C_nA_p$ to show that the doping level is proportional to salt concentration regardless of the charge of salt cations or anions (see Supporting Information).

The second significant prediction[12] is that the PEMU concentration of the ferrocyanide probe species, $\bar{C}$, is independent of $[\mathrm{NaCl}]_{aq}$ and, from eq 5, independent of $y$. Generally, for probe ion $F$ of charge $\nu^-$ (see Supporting Information)

$$\bar{C} = [\mathrm{Pol}_\nu^{\nu+}F^{\nu-}]_m = k'[F^{\nu-}]_{aq} \tag{6}$$

where $k'$ is a constant. The invariance of the probe ion concentration with salt is a unique feature of the reluctant exchange mechanism. It reflects the tendency for additional salt to *create* ion exchange sites, balanced by a tendency for salt to *occupy* these sites. In classical Donnan exchangers, salt would compete with probe ion for fixed sites, decreasing $\bar{C}$.

The two critical properties of the reluctant exchanger—dependence of doping level on salt according to eqs 4 and 5 and constancy of $\bar{C}$—have not previously been directly experimentally verified. Dimensional changes during swelling were used to indirectly estimate a value for $K_1$.[13] In the present work, an in situ spectroscopic method was employed to follow the population of salt ions within a PEMU.

## Results and Discussion

A multilayer of poly(diallyldimethylammonium) (PDADMA) and poly(styrene sulfonate) (PSS), terminated with PSS to avoid Donnan inclusion of anions,[16] was deposited on the surface of a crystal used for attenuated total internal reflection infrared spectroscopy (ATR-FTIR).[25] The thickness of the PEMU (~3 $\mu$m) was such that the evanescent wave[25] (~0.6 $\mu$m at 1000 $cm^{-1}$ for the system described) emanating from the ATR crystal (germanium) was contained completely within the PEMU. Thus, when placed in a flow cell, only signals from species *within* the multilayer were detected. The strong sulfonate stretches of PSS were used as a convenient internal standard to obtain accurate and precise measurements of salt ion within PEMU.

Figure 1 depicts $y$ as a function of the activity of $NaClO_4$ solution (lacking infrared activity, NaCl could not be used) contacting the PEMU, converted from $[NaClO_4]_{aq}$ with the appropriate activity coefficient[26] using the strong $ClO_4$ vibrational mode at 1100 $cm^{-1}$ to determine the fraction of $Pol^+ClO_4^-{}_{(m)}$ (the doping level). There are several significant findings relevant to PEMUs, and stoichiometric polyelectrolyte complexes in general, to be gleaned from Figure 1. First, a small population of trapped residual persistent extrinsic charge, $y_{rpe}$, is observed as $a_{NaClO_4} \rightarrow 0$. For the reluctant mechanism to dominate, $y_{rpe}$ should be negligible. The multilayer for Figure 1 had been previously annealed for 24 h in 1 M salt. Considerably more $y_{rpe}$ (approaching $y = 0.1$) was observed for as-made PEMUs that were not annealed in this way. Prior studies with radioisotope salt ions,[4] establishing an upper limit

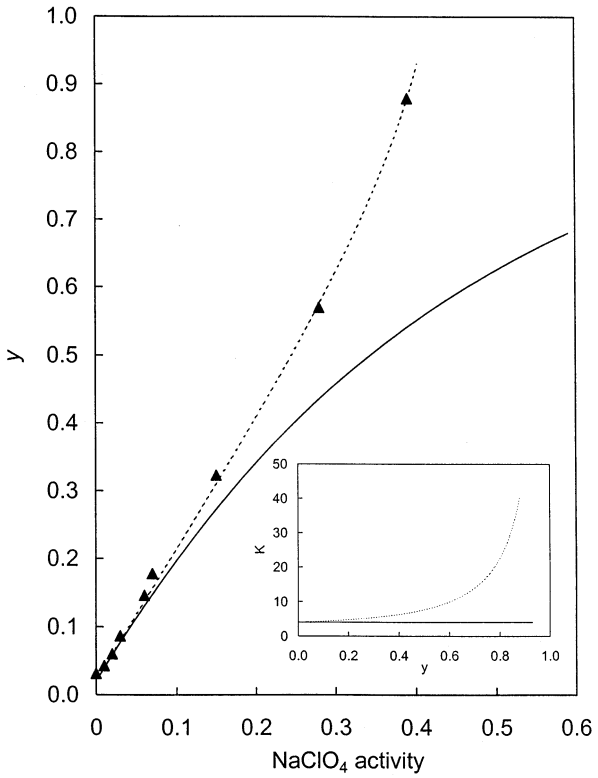


***Figure 1.*** Doping level, $y$, for perchlorate ion as a function of solution $NaClO_4$ activity, measured in situ with ATR-FTIR for a 3.1-$\mu$m-thick (measured by profilometry in the dry state) PSS/PDADMA multilayer on germanium. The solid line is a theoretical fit of $y$ to $NaClO_4$ activity according to eq 4, assuming a constant value of 4 for $K_1$. The dotted line is the same fit but with $K_1$ varying with $y$ according to the inset. The multilayer decomposes for $NaClO_4$ activities greater than ~0.4.

of a few ppm for $y_{rpe}$, were performed with much thinner, well-annealed PEMUs. Clearly, postdeposition handling and processing of multilayers figures strongly in $y_{rpe}$. Given that time and salt are needed for effective annealing,[13] it may be possible to maximize trapped extrinsic charge for low-salt concentrations and rapid deposition, encouraging layering, orientation, or both.

A second notable finding is the instability of the multilayer to $NaClO_4$ activities beyond 0.4. At this point, $y$ approaches 1. As expected, for activities greater than ~0.4, where $y$ would be (a physically impossible) >1, the multilayer decomposed (no IR signal from PEMU was observed) as all polymer–polymer contacts were broken. This critical salt concentration for multilayer decomposition[27] varies strongly with polyelectrolytes and salt type. For example, a "clean" and rapid decomposition was observed for a poly(acrylic acid)/PDADMA multilayer for $[NaCl]_{aq} > 0.6$ M at room temperature,[27] whereas PSS/PDADMA is stable up to ~3.5 M NaCl.

The fit of experimental data in Figure 1 to eq 4 with a single value of $K_1$ (solid line) is satisfactory at low $y$ but shows strong deviation as $y \rightarrow 1$. Much better fitting over the whole range is obtained if $K_1$ is assumed to vary with $y$ according to the inset in Figure 1. The variation of $K_1$ is modeled by

$$K_1 = K_o - 1 + \frac{1}{1-y}e^{hy} \tag{7}$$

with $K_o$ and $h$ fitting parameters (for Figure 1, respective values

(25) (a) Harrick, N. J. *Internal Reflection Spectroscopy*; Interscience: New York, 1967. (b) Urban, M. W. *Attenuated Total Reflectance Spectroscopy of Polymers*; American Chemical Society: Washington, 1996.
(26) Dobos, D. *Electrochemical Data, A Handbook for Electrochemists in Industry and Universities*; Elsevier SPC: New York, 1975.
(27) Dubas, S. T.; Schlenoff, J. B. *Macromolecules* **2001**, *34*, 3736.

of 4 and 1.7 were satisfactory). Equation 7 is an empirical description of how $K_1$ depends on $y$. Variation of $K_1$ as a function of $y$ is an indication that polyelectrolyte binding is cooperative[28,29] and that the formation constant (inverse of $K_1$) for complexation, on a per segment basis, increases at higher degrees of association, but a limit is reached at sufficiently associated (low $y$) levels where cooperativity plateaus. Although cooperativity as a function of chain length is well known in polyelectrolyte complexation, and is known to be driven by the same entropic considerations as the "ligand effect," for example,[30] the degree of association within preformed complexes as a function of salt has only recently started to be probed.[31]

Cooperativity for polymer associations can be understood in the following way: each binding event incurs a configurational and translational entropy penalty, both for the polymer segment and for its attendant counterions and waters of hydration. As $y$ decreases, each segment loses fewer degrees of freedom on association, making binding more favorable in comparison to earlier binding events at higher $y$. It is seen that $K_1$ is effectively constant for $y$ up to ~0.3. This is reasonable, since, for $y$ lower than 0.5, on average each extrinsic site on a chain is already surrounded by two intrinsic sites, which represents the limit of cooperativity. The interesting nonlinear control of ion transport discussed below occurs at low $y$, where both the constant value $K_1$ and $y \sim$ [salt] (eq 5) approximations are valid.

Further consideration of the very rapid increase in $K_1$ near $y = 1$ leads to one final conclusion. If $K_1$ were constant, $y$ would have a finite value even for very high salt concentrations. High molecular weight polyelectrolytes would still be associated, network style, perhaps enough to strongly impact solution properties. Because of the rapid increase in $K_1$, polymer molecules "let go" of each other at lower values of $y$ and physically reasonable salt concentrations. Full dissociation of polyelectrolyte complexes is thus possible.[19,27,32,33] Figure 1 approaches an association/dissociation phase transition that will probably have a very low dependence on molecular weight for degrees of polymerization greater than ~10.[34]

The second critical feature of the reluctant exchange mechanism, the constancy of $\bar{C}$, was also verified experimentally with in situ ATR-FTIR. The membrane concentration of the probe ion was determined as $[NaCl]_{aq}$ varied while the solution concentration of the probe was held constant. Here, ferricyanide could not be used, since it was reduced to ferrocyanide by the germanium crystal, and ferrocyanide took too long to equilibrate through the thick film. Instead, cobalticyanide, $Co(CN)_6^{3-}$, at a concentration of 1 mM, was employed, using the CN stretch at 2130 $cm^{-1}$ to quantify the anion within the PEMU. As seen in Figure 2, $\bar{C}$ is, indeed, constant. $\bar{C}$ for cobalticyanide is presented as a mole ratio compared to sulfonate, used as the internal standard. This strategy normalizes variations in the absolute absorbance due to changes in refractive index and density as the salt swells the multilayer. Using a concentration of ~2 M for sulfonate groups in the swollen PEMU, $\bar{C}_{cobalticyanide}$ is ~0.07 M.

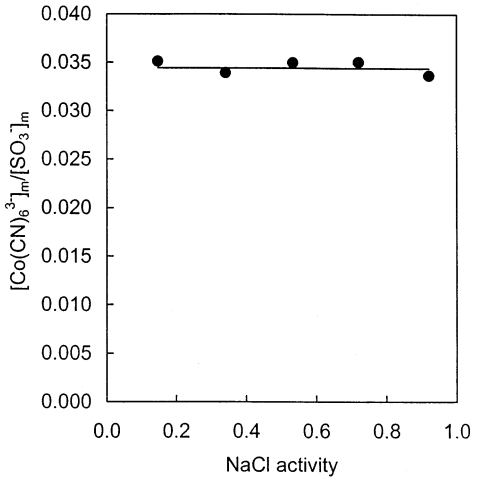


***Figure 2.*** Multilayer (PSS/PDADMA) concentration of cobalticyanide probe ion, normalized to polymer sulfonate (internal standard), as a function of the solution activity of salt. The solution concentration of $Co(CN)_6^{3-}$ was 0.001 M in all cases.

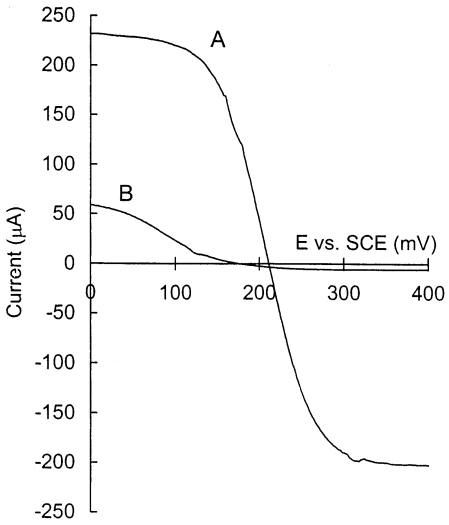


***Figure 3.*** Linear sweep voltammograms of a mixture of 0.001 M ferricyanide and 0.001 M ferrocyanide in 0.6 M salt at a platinum rotating disk electrode. Curve A was obtained with a bare electrode. For curve B, the electrode was coated with a 70-nm-thick PSS/PDADMA multilayer. Rotation rate, 1000 rpm; scan rate, 10 mV $s^{-1}$; Pt disk diameter, 8 mm; reference electrode, saturated calomel.

**Diffusion through an Exchanger Membrane.** Having established the equilibrium distribution of ions through a PEMU, we now address the control of transport of an electrochemically active "probe" ion by (electrochemically inactive) salt ions, present at much higher concentration, corresponding to eqs 4−6.

Linear scan voltammograms of an equimolar mixture of (electrochemically active) ferro- and ferricyanide at a rotating platinum disk electrode (RDE) are depicted in Figure 3. Both bare and multilayer membrane-coated electrodes are represented. Classical S-shaped steady-state voltammograms with plateaus at the convection−diffusion-limited currents[35] are observed. Positive (reduction) currents are attributed to the flux of ferricyanide, and negative (oxidation) currents are due to

(28) Tsuchida, E.; Osada, Y. *Makromol. Chem.* **1974**, *175*, 593.
(29) Yu, S. Y.; Hirata, M.; Chen, L.; Matsumoto, S.; Matsukata, M.; Gong, J. P.; Osada, Y. *Macromolecules* **1996**, *29*, 8021.
(30) Cohen Stuart, M. A. In *Short and Long Chains at Interfaces*; Daillant, J., Guenoun, P., Marques, C., Muller, P., Trân Thanh Vân, J., Eds.; Editions Frontières: Gif-sur-Yvette, France, 1996; pp 1−12.
(31) Křiž, J.; Dybal, J.; Dautzenberg, H. *J. Phys. Chem. A* **2001**, *105*, 7486.
(32) Michaels, A. S.; Miekka, R. G. *J. Phys. Chem.* **1961**, *65*, 1765.
(33) (a) Sukhishvili, S. A.; Granick, S. *J. Am. Chem. Soc.* **2000**, *122*, 9550. (b) Sukhishvili, S. A.; Granick, S. *Macromolecules* **2002**, *35*, 301.
(34) $K_1$ is the equilibrium swelling constant for a segment. The inverse, $K_1^{-1}$, is the association constant per segment, but not the association (formation) constant for the entire macromolecule. The latter scales approximately as $e^n$, for small $n$, where $n$ is the number of repeat units. See refs 28 and 30.

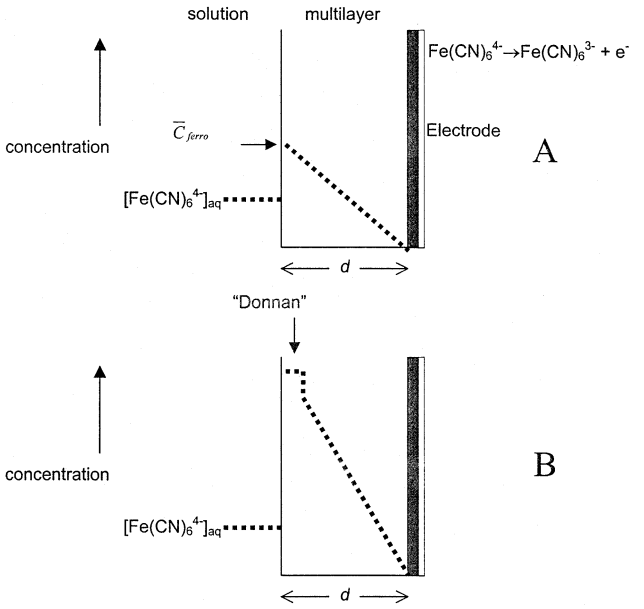


***Figure 4.*** Schematic concentration gradients of ferrocyanide through a multilayer coating an electrode surface at the limiting current. $[Fe(CN)_6^{4-}]_m \rightarrow 0$ at the electrode surface and is given by an equilibrium constant at the PEMU/solution interface. In (A), the profile is depicted by assuming a homogeneous reluctant exchanger distribution of probe ion at $i_m = 0$. The membrane/solution partition coefficient is ~2. In (B), the presence of a thin layer of positive excess surface polymer charge causes inclusion of $[Fe(CN)_6^{4-}]$ into the multilayer surface and a corresponding increase in the concentration profile, giving higher $i_m$. The system is assumed to be at the "well-stirred" limit, where mass transport is limited mainly by diffusion through the film and not by diffusion through the stagnant layer of liquid adjacent to the PEMU.

ferrocyanide. It is clear that although the fluxes of ions in solution are similar (they have similar aqueous diffusion coefficients), the flux (current) of ferricyanide through the membrane is significantly higher than that of ferrocyanide.[36]

Mass transport through the PEMU is purely diffusive. The salt concentration (extrinsic site concentration) within the multilayer is higher than that of the probe ion. The mobility of salt ions is also much higher, since they are singly charged (vida infra). The role of salt as supporting electrolyte is typical in suppressing the electric field within the PEMU and external to it, therefore minimizing field-driven migration of redox probe.[35] Though polymeric PEMU components are highly ionic, they are virtually immobile (in contrast to small ions) and unable to participate in charge transport.

At the limiting currents, boundary conditions are as follows:[16] the concentration of probe ion is zero at the electrode surface (all material is consumed at the diffusion-limited rate); the membrane concentration of probe at the electrolyte/PEMU interface is constant (and given by an equilibrium distribution or partition coefficient). The resulting concentration profiles are depicted in Figure 4, which shows no (significant) concentration gradient in the stagnant layer of electrolyte adjoining the membrane. Such an assumption is valid for "well-stirred" systems.[20] The stagnant aqueous layer is much thicker (~15 $\mu$m) than the typical PEMU. Using limiting currents for bare electrodes, contributions to resistance to mass transfer through the stagnant film may be precisely removed[12,37] from the overall mass-transfer resistance to yield the membrane-limited current, $i_m$, and corresponding flux, $J_m$, of probe ion

$$J_m = i_m/nFA = \bar{D}\bar{C}/d \tag{8}$$

where $\bar{D}$ and $\bar{C}$ are the respective membrane diffusion coefficient and concentration of the probe ion, $d$ is the multilayer thickness, $A$ is the electrode area, $n$ is the number of electrons transferred (1 in this case), and $F$ is Faraday's constant (96 490 C mol$^{-1}$).[20] Hereafter, we refer only to membrane flux, $J \equiv J_m$, extracted from limiting currents as described previously.[12,37]

Equation 8 clearly shows that flux may be enhanced by increasing $\bar{D}$ or $\bar{C}$. If the multilayer bears a net positive polymer surface charge, negative ions are included into the surface by the classical Donnan action.[16] The enhanced surface concentration leads to greater $\bar{C}$, as depicted in Figure 4, and higher flux (currents), as found previously.[12,38] We term this interesting example of cooperative surface classical exchanger and bulk reluctant exchanger "Donnan enhancement" of flux. The importance of this mechanism for amplifying signals from dilute solution species should not be overlooked. The PEMU literature contains other examples of "surface effects" with apparently mysterious long-range consequences within the multilayer.[39,40] A surface layer is capable of modifying the chemical potential of a species within the whole PEMU in a manner similar to Donnan enhancement. In general, s*urface composition may be critical in determining bulk properties* of PEMUs. A quantitative treatment of the Donnan effect due to surface charge has been provided recently.[41] We emphasize that, for sufficiently thick films (more than 6−7 layers), the nonlinear flux response to salt concentration was *still* observed for Donnan-enhanced PEMUs. Clearly, despite surface charge inclusion of probe ion, reluctant exchange throughout the bulk of the film is still a controlling mechanism.

**Empirical Scaling for Membrane Flux.** Salt moderates the permeation of probe ions of different charge to different extents. Figure 5 presents $i_m$ for a collection of redox-active ions with charges ranging from 0 to 4. While the flux of all charged species is moderated by salt, probes of higher charge exhibit lower flux, as observed by other researchers.[8d,42] In addition, the dependence of flux on salt concentration is strongly nonlinear. For an ion of charge $\nu$, we observe the following empirical scaling dependence

$$J \sim [NaCl]_{aq}^{\nu} \tag{9}$$

Having established that $\bar{C}$ is constant, we look to $\bar{D}$ and $d$ from eq 8 as the two remaining controlling factors. The thickness is linearly related to the doping level and, for the present analysis, is assumed to be pseudoconstant ($d$ increases by ~10% in the

(35) Bard, A. J.; Falkner, L. R. *Electrochemical Methods*, 2nd ed.; Wiley: New York, 2001.
(36) Adapting the treatment for the shape of a voltammetric wave (Chapter 9 in ref 35), the position of the half-wave potential should be $E_{1/2} = E^{o'} + RT/nF \ln(D_{ferro}/D_{ferri})$. $E^{o'}$ was ~180 mV vs SCE, ~95 mV more positive than $E_{1/2}$ for the coated electrode wave in Figure 3, which places the ratio of $D_{ferri}/D_{ferro}$ at ~40.
(37) (a) Gough, D. A.; Leypoldt, J. K. *Anal. Chem.* **1979**, *51*, 439. (b) Ikeda, T.; Schmehl, R.; Denisevich, P.; Willman, K.; Murray, R. W. *J. Am. Chem. Soc.* **1982**, *104*, 2683.
(38) Lvov, Y. In *Protein Architechure. Interfacing Molecular Assemblies and Immobilization Biotechnology*; Lvov, Y., Möhwald. H., Eds.; M. Dekker: New York, 2000.
(39) Schwarz, B.; Schönhoff, M. *Langmuir* **2002**, *18*, 2964.
(40) Xie, A. F.; Granick, S. *J. Am. Chem. Soc.* **2001**, *123*, 3175.
(41) Calvo, E. J.; Wolosiuk, A. *J. Am. Chem. Soc.* **2002**, *124*, 8490.
(42) Harris, J. J.; Stair, J. L.; Bruening, M. L. *Chem. Mater.* **2000**, *12*, 1941.

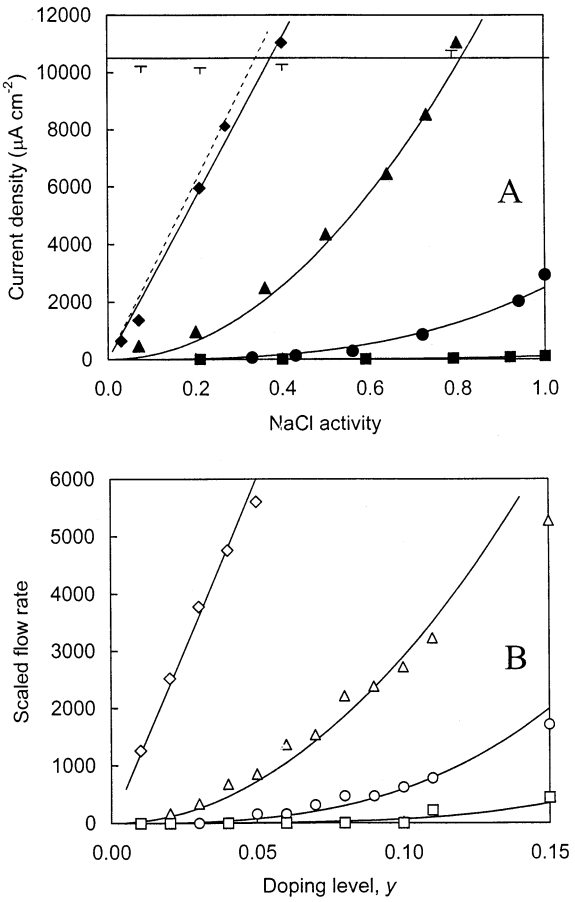


***Figure 5.*** (A) Membrane limiting current densities, $j_m$, at a multilayer-coated RDE vs solution salt activity, of 0.001 M solutions of hydroquinone (crosses), iodide (diamonds), $Fe^{2+}$ (triangles), ferricyanide (circles), and ferrocyanide (squares) representing, respectively, probe ions of charge, $\nu = 0, 1, 2, 3, 4$. The solid lines are respective fits to empirical scaling $j_m \sim a_{NaCl}{}^{\nu}$. The dotted line represents $j_m$ for $I^-$ corrected for swelling of the multilayer. Twenty-layer PSS/PDADMA of thickness 70 nm, surface neutralized by PSS; 22 °C; 1000 rpm rotation rate. (B) Scaled flow rate vs doping level, $y$, for a Monte Carlo simulation of ion hopping with ions of charge 1 (diamonds), 2 (triangles), 3 (circles), and 4 (squares). The solid lines represent empirical power law scaling. For the simulation, the lattice was 500 × 400, the hopping distance was 2 lattice units. The size of the area in which the appropriate number of extrinsic sites must appear ($b$) was 8 lattice points. Five simulations were averaged for each point. Probe ion concentration was 5000 of the 200 000 available lattice points.

present case for the salt concentration range in Figure 5.[13] For $I^-$, a correction for swelling is shown). There are examples of very strong swelling (large $K_1$'s).[13] In this limit, the membrane has little measurable barrier effect. If $d$ is constant, all changes in $J$ can be ascribed to changes in $\bar{D}$, and since $y \sim [NaCl]_{aq,lim[NaCl]\to 0}$, we obtain the following scaling behavior

$$J \sim y^{\nu} \tag{10}$$

With multivalent salt $M^{q+}Cl_q$ and negative probe ion, the $J \sim y^{\nu}$ scaling still holds, (as experimentally verified with $CaCl_2$, $MgCl_2$, and $YCl_3$ as salt and the ferro/ferricyanide system) because singly charged chloride still serves as the negative salt ion balancing extrinsic cationic sites, which are sought out by ferro/ferricyanide. The overall flux is found to be higher because $K_1$ is larger. If the salt contains ions, charge $q$, of the same sign as the probe ion, we expect $J \sim y^{\nu/q}$ (and $J \sim [salt]^{\nu/q}$) because the salt ions now enforce greater coincidence of extrinsic sites as required by the mechanism below. In the present work, our experimental and theoretical treatments are limited to univalent salt.

**Hopping Model.** The mechanism of transport posited is one of ion hopping between discrete sites. These sites are small clusters of extrinsic polymer charges coupled to counterions. Any ion, be it a salt or a probe ion, is associated with a particular oppositely charged polymer segment. This is a rather un-Debye−Hückel (DH) statement: in the high ionic strength limit, charges should be heavily screened and oblivious of each other.[43] However, DH theory is valid for dilute ionic strength and assumes a mean field for the electrostatic potential experienced by a point charge in the presence of others.[43] We assert that the polymer charges within the PEMU are discrete and recognizable as such by counterions. This disposition of ions within the multilayer—counterions paired with polymer segments—contrasts with another where salt simply exists in "pools" of water, in which case, transport should be of the pinhole type.[37]

While it would be experimentally difficult to observe directly whether a salt counterion resides next to a polymer segment or another counterion, several observations point toward an ion pairing association: first, pinhole behavior in these PEMUs has been previously discounted;[12] second, the nonlinear enhancement of flux and scaling with charge is not explained by transport through pools or channels of water; and finally, specific ion pairing effects are seen. The latter category includes the dependence of the swelling constant, $K_1$, on ion type. For example, swelling by perchlorate is much more efficient than swelling by chloride (compare Figures 1 and 5), indicating preferred ion pairing of perchlorate with PDADMA. Further evidence that ions are coupled to segments as in eqs 1 and 2, rather than "dissociated" as observed for solution species, is provided by the observation that salt ions moderate the dissociation of weak acids within multilayers.[14] DH theory does not explain the increase in thickness with salt[6] and cannot account for the differences in swelling for different multilayers.[13]

Viewed at the molecular level, hopping is actually an ion exchange: $\nu$ extrinsic charges occupied by salt counterions are now replaced by a probe ion, and the vacancies that appear as a result of the departure of the probe ion are occupied by salt ions. At some point in this transaction, there is a momentary charge separation of ion from fixed site. Motion of this kind should be thermally activated, and the appropriate temperature dependence has been observed previously.[12] The high dielectric constant of the medium (several water molecules per intrinsic or extrinsic site are present) assists charge separation. An ion exchange hopping, where salt and probe ions change place, implies the movement of both species are coupled. The coupled interdiffusion of two different anions, A and B, diffusion coefficients $\bar{D}_A$ and $\bar{D}_B$, and charges $z_A$ and $z_B$, for respective membrane concentrations $\bar{C}_A$ and $\bar{C}_B$, can be described in terms of one diffusion coefficient $\bar{D}_{AB}$ by[16]

$$\bar{D}_{AB} = \frac{\bar{D}_A\bar{D}_B(z_A{}^2\bar{C}_A + z_B{}^2\bar{C}_B)}{z_A{}^2\bar{C}_A\bar{D}_A + z_B{}^2\bar{C}_B\bar{D}_B} \tag{11}$$

From eq 11, it is evident that the slower ion present at lower concentration will have a stronger effect on interdiffusion. With

(43) Radeva, T., Ed. *Physical Chemistry of Polyelectrolytes*; M. Dekker: New York, 2001.

ferro/ferricyanide and chloride from NaCl, these criteria are certainly met. In other words, with ions A and B represented by ferri(o)cyanide and chloride from salt, respectively, $\bar{D}_{AB} \rightarrow \bar{D}_A$.

Charge hopping as applied to electron transport is a well-known phenomenon.[18] In soft condensed matter, charge can be transported by physical diffusion of probe (as occurs here) or electrons can tunnel between sites of mixed oxidation state (mixed valence). For example, both "redox" polymers[21] (where charge resides on metallic centers) and doped conjugated polymers[20] (where charge is delocalized over several conjugated repeat units and conductivity is favored in the chain direction) exhibit electron hopping. Where ion movement and electron hopping coexist, it is possible to freeze out the former and obtain ohmic transport driven by electric fields.[21i] This possibility has been considered in detail and discounted for the present system.[12] The points of departure of the present system from classical electron hopping are 2-fold: first, "doping" does not change the density of redox centers within the polymer ($\bar{C}$ is constant); second, because ions may be multiply charged (as opposed to the electron), an unusual nonlinear dependence on doping level is observed.

The diffusion coefficient for hopping transport in two dimensions is given by[44]

$$D = \delta^2/4\tau \tag{12}$$

where $\delta$ is the average hopping distance and $\tau$ is the hopping time. (The difference between two-dimensional and three-dimensional diffusion is the denominator is $6\tau$ in the latter case. This does not affect the scaling behavior). The membrane flux may be written as

$$J(y,v) = \frac{\bar{D}\bar{C}}{d} = \frac{\delta^2 k_{o,hop} P(y,v)\bar{C}}{4d} \tag{13}$$

The hopping time has been replaced by a hopping attempt frequency, $k_{o,hop}$,[45,46] and the probability $P(y,v)$ that an attempt will be successful. $k_{o,hop}P(y,v)$ is the observed hopping rate. When $P = 1$, every attempt is successful and ions flow at their maximum rate. This simple expression assumes all parameters remain constant except $P$. Such an assumption has been verified explicitly for $\bar{C}$ and $\delta$. $k_{o,hop}$ should be thermally activated and thus constant at constant temperature.

**Monte Carlo Simulation (MCS).** A hopping transport model can be simulated to obtain a value of $P$ for various values of probe charge and membrane doping level. The problem is exemplified by Figure 6, which shows a triply charged probe ion, balanced by three univalent extrinsic sites, attempting to hop under five scenarios. Each hopping attempt results in either failure or success. The large dashed circle represents a hopping range and, the small dashed circles represent a "site"−an area of $b$ adjacent lattice points within which the probe must find at least three extrinsic charges available to maintain electroneutrality. Only one hopping attempt in Figure 6 is successful. Attempt **a** fails because the site is already occupied. (Self-exchange is possible but does not lead to net displacement.) Attempts **b** and **c** fail because there are, respectively, no, or insufficient, extrinsic charges. Site **d** is out of the hopping range. Only site **e** has three unoccupied (by probe) extrinsic charges within the hopping range.

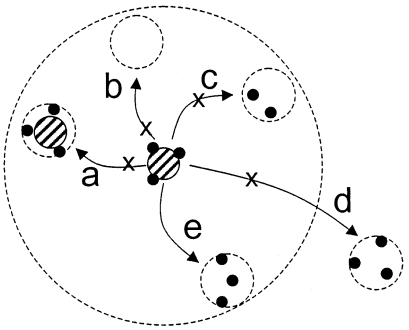


***Figure 6.*** Boundary conditions for hopping model. A probe ion of charge 3 (shaded circle) is balanced by three oppositely charged extrinsic sites (solid). The hopping range is represented by the large dotted circle. The area in which at least three extrinsic charges must appear (a "site") is given by the small dotted circle. Of the five hopping attempts depicted, only (e) is successful in finding an unoccupied (by probe ion) site with at least three charges within the hopping range.

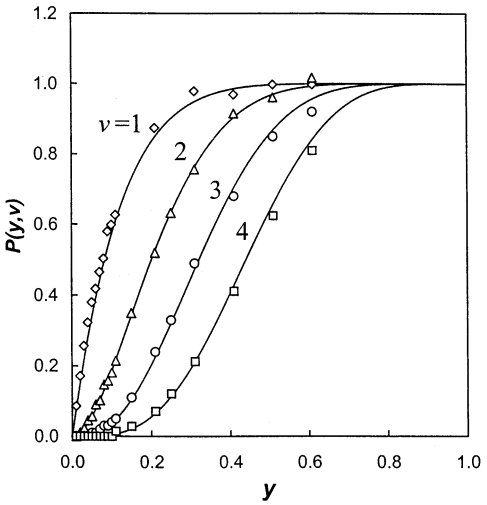


***Figure 7.*** Probability function, $P$, vs doping level, $y$, for $v$ from 1 to 4 and $b = 8$. A nonlinear region at low $y$ (for $v > 1$), followed by saturation, is evident. Values of $P$ from both Monte Carlo simulations (open symbols) and the continuum probability model (solid lines) are shown.

In the MCS a two-dimensional grid is set up that is 500 lattice units high and 400 units wide. The width of the grid represents the thickness of the PEMU. A simulation step consists of introducing a fixed number of extrinsic charges, randomly distributed (compensated by salt ions in the real system), and observing the hopping response of a more dilute population of probe ions. The hopping probability, $P$, for a simulation step is calculated by dividing the number of probe ions that have hopped by the total number of probe ions. Many simulation steps are averaged for good statistics. Values of $P$ as a function of $y$ are given in Figure 7. While individual probe ions are tracked as a function of time, the extrinsic sites are not, since this would be computationally too intensive. However, in the limit of fast extrinsic site diffusion, introducing a random distribution of extrinsic sites on each simulation step is valid here.

(44) Egelstaff, P. *An Introduction to the Liquid State*; Academic Press Inc.: New York, 1967; Chapter 10, pp 119−132.

(45) $k_{o,hop}$ represents those attempts at hopping that have sufficient energy to be successful if sites were available to receive the ion. Insufficiently energetic molecular motions are not considered "attempts" within the current framework.

Because several parameters, such as hopping distance, attempt frequency, and concentration of extrinsic and intrinsic sites, are unknown, the model will *only* provide scaling behavior. The flux is normalized so that the *y*-axis matches the corresponding units in the experimental data set. In Figure 5, MC simulations have been presented only up to the *y* values where they correlate with "empirical scaling" (low *y*). A more extended range is presented later. As seen in Figure 5, the empirical scaling behavior is reproduced by the MCS at low *y*. If the probe ion is consumed as it reaches one side of the simulation grid, as would be the case in an electrochemical experiment, the concentration of probe ion would be nonuniform. The expected time-dependent and steady-state (Figure 4) concentration profiles[44] were reproduced by MCS (see Supporting Information).

**Continuum Probability Model.** Using a minimal set of boundary conditions, Monte Carlo simulations enable one to visualize the transport as it is occurring and, for example, generate concentration profiles. Disadvantages are that MCS is computationally intensive, produces inherent statistical errors from the limited size of the data set, and only yields one point for each set of simulation conditions. Using the same ideas presented in Figure 6, a hopping attempt will be successful *only* if the probe ion finds *at least* $\nu$ extrinsic charges at the location to which it tries to hop. In a combinatorics approach, the problem is reduced to the probability of finding at least $\nu$ sites clustered together at a given doping level.

We define $b$ as the number of lattice points comprising a small area $B$, wherein the probe ion must find at least $\nu$ extrinsic charges. Realistically, $b$ is likely to be a small number reflecting short-range interactions between probe and neighboring extrinsic sites. The statistical treatment yields the following binomial expression for the probability of finding *exactly* $\nu$ sites within area $B$ made up of $b$ adjacent lattice points given doping level $y$ (details of the statistical treatment are provided in Supporting Information):

$$P(\nu \in B) = \binom{b}{\nu} \cdot y^{\nu} \cdot (1-y)^{b-\nu} \tag{14}$$

where $0 \leq \nu \leq b$ and the term in parentheses is the binomial coefficient. The probability of finding *at least* $\nu$ sites within $b$ lattice points is

$$P(\geq \nu \in B) = \sum_{\nu}^{b} \binom{b}{\nu} \cdot y^{\nu} \cdot (1-y)^{b-\nu} \tag{15}$$

In the $y \ll 1$ limit, the probability function in eq 15 can be approximated to

$$P(\geq \nu \in B) \approx \binom{b}{\nu} \cdot y^{\nu} \tag{16}$$

reproducing the empirical scaling observations. For example, if $b = 8$ and $\nu = 3$, eq 16 would yield $P = 56y^3$.

In Figure 7, $P(y,\nu)$ for probe ions of different charge is presented over the whole range of $y$ for $b = 8$ The nonlinear scaling at low $y$, followed by saturation at high $y$, is evident. Agreement with $P$ values from MCS is very good. In Figure 8, scaling comparisons between the three models, empirical, MCS, and continuum probability, are presented. All three models are similar at low $y$, and the latter two coincide to high doping levels. Interestingly, the deviation from empirical scaling occurs at higher doping levels for ions of greater charge. For comparison, experimental $J_m$ versus salt data to high-salt concentration are also presented in Figure 8. Evidence of saturation is seen. In comparing the experimental current versus $[NaCl]_{aq}$ data with any of the theoretical scaling plots of flux versus $y$, it should be remembered that $y$ is a linear function of $[NaCl]_{aq}$ only at low $y$. A dependence of $K_1$ on $y$ (Figure 1) fortuitously makes this proportionality continue to somewhat higher $y$ than if $K_1$ had been constant.

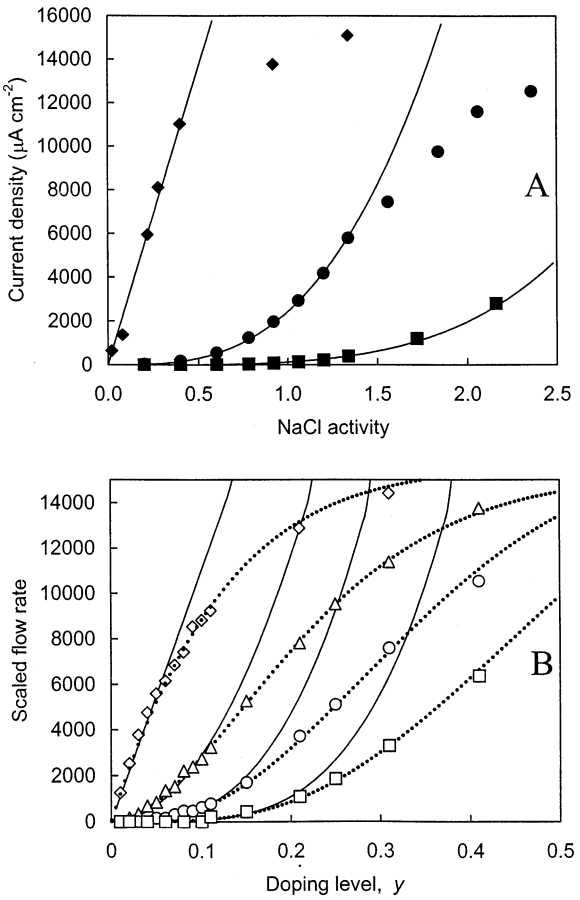


***Figure 8.*** (A) Membrane limiting current densities, $j_m$, at a multilayer-coated RDE vs solution salt activity, of 0.001 M solutions of iodide (diamonds), ferricyanide (circles), and ferrocyanide (squares) to high salt activity. The rest of the experimental conditions as in Figure 5A. (B) Combined empirical scaling (solid lines), MCS (points), and continuum probability (dotted line) plots for the scaling of membrane flux with doping level for $\nu = 1$ (diamonds), $\nu = 2$ (triangles), $\nu = 3$ (circles), and $\nu = 4$ (squares).

Certain refinements to the hopping model are possible. Our treatments assume that both $\delta$ and $k_{o,hop}$ are constants. The hopping distance represents an average but is not likely to be more than ~20 Å. As $y \rightarrow 1$, more short-range sites will be available, encouraging transport, delaying saturation, and keeping flux nonlinear to higher $y$. $k_{o,hop}$ will likely have a thermally activated Arrhenius-type dependence on temperature. This activation energy barrier, if it is to be measured by flux dependence, must be separated from temperature-induced changes in $\bar{C}$ (through $K_1$). Direct methods for measuring hopping rate, such as NMR to determine relaxation times, may be more reliable than flux measurements.[47] It is anticipated that

(46) Crank, J. *The Mathematics of Diffusion*; Clarendon Press: Oxford, U.K., 1975; p 1967.

information on segmental and ionic motion obtained using NMR will be extremely useful in estimating hopping rates and in guiding molecular dynamics simulations.

We have not considered "low-salt" conditions, where the only source of ionic strength is from added probe ions themselves. This example of "autodoping" is more like classical doping, where the "dopant" provides both a site ("defect") and a mobile charged species (electron or hole). In this case, $y \sim \bar{C} \sim [F^{\nu-}]$, $\bar{D}$ is likely to scale with $[F^{\nu-}]$, so $J \sim [F^{\nu-}]^2$ for small $y$. In the absence of salt, however, the electrochemistry would be nonideal, with contributions from both diffusion and electric field (migration) transport.

**Flux Selectivity.** From the foregoing theoretical treatments, it is clear that probe ions of higher charge will have a lower probability of hopping since they require greater coincidences of extrinsic charge within the multilayer. Flux selectivity, preferring ions of lower charge, is expected from this constraint. Further, since the scaling relationships depend on ion charge, the actual magnitude of the selectivity will depend on the doping level. Tunable selectivity would be an attractive membrane property. For example, the flux selectivity for hydroquinone over ferrocyanide is 5000 at $a_{NaCl} = 0.1$ (Figure 5), but the selectivity drops to 5 at $a_{NaCl} = 2.0$ (Figure 8). On the plus side, the flux for both increases at higher salt concentration. One is presented with a rational way of making the flux versus selectivity tradeoffs that are common in membrane separations.

Figure 9 compares the experimental and simulated flux ratios for the ferri/ferricyanide systems diffusing through PSS/PDADMA. A wide range of selectivity is available. The *x*-axes have been presented as shown because we have established, for PSS/PDADMA, the following approximate relationship for doping level versus activity of salt: $y = 0.2a_{NaCl}$.[13] Selectivity is higher than predicted based solely on charge. Factors other than statistical ones will control transport of species through PEMUs. For example, greater membrane concentrations ($\bar{C}$) will lead to higher $J_m$ (eq 8). Other factors such as attempt frequency or hopping distance (eq 13) will also come into play. We have found that larger, more hydrophobic ions move more slowly than others of the same charge. Preliminary results[12] indicate $\bar{C}$ for ferricyanide is larger than that for ferrocyanide (contrary to the "rule" for classical ion exchangers that the exchanger prefers species of higher charge[16]), but the difference is insufficient to explain the 7-fold discrepancy between experimental and simulated selectivities in Figure 9. It is likely that because more highly charged species require more segment reorganization the hopping activation barrier is higher, and $k_{o,hop}$ is lower. In other words, more energy is required for a successful hop. Some treatment similar to the Marcus theory for electron transfer might be illuminating here.

## Conclusions

A theoretical basis for rationalizing hopping transport of ions within polyelectrolyte multilayers has been developed and correlated with experimental data. Including the systems described herein, we have, to date, performed salt-controlled permeability studies with combinations chosen from approximately 15 electrolytes, 10 probe ions, and 20 pairs of polyelectrolytes. The overall fit to theory and self-consistency within these systems is satisfactory at the level of sophistication presented. PEMUs are amorphous, homogeneous blends of constituent polymers and ions with no "grain boundaries"—properties that simplify the analysis.

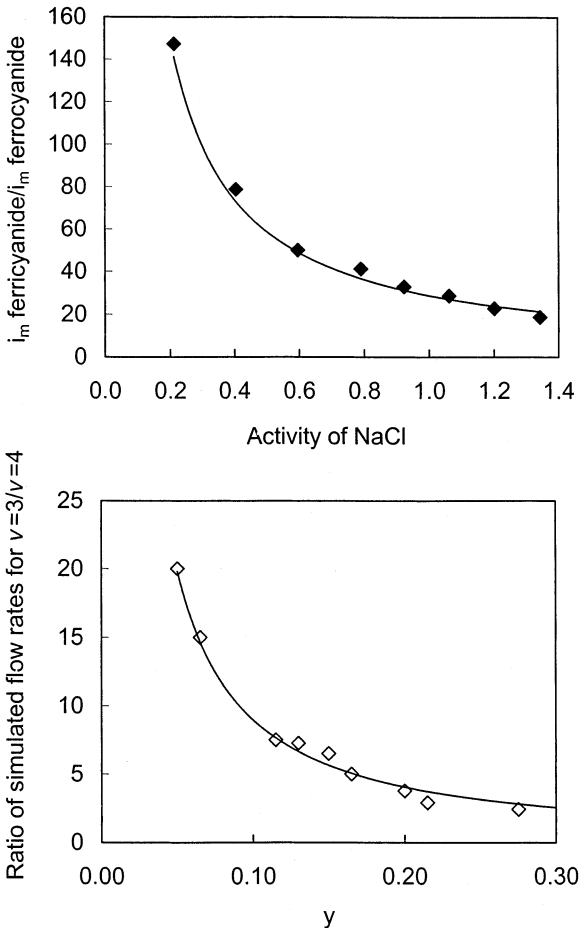


***Figure 9.*** Upper panel: ratio of the experimental membrane currents (flux selectivity) for ferri- vs ferrocyanide from Figure 5A. Lower panel: ratio of the Monte Carlo simulated fluxes for $\nu = 3$ and $\nu = 4$ from Figure 5B (assumes membrane concentration for both is the same). Solid lines are from ratio of empirical scaling.

Implications for ion transport are several. The nonlinear control of minority ion mobility by majority ion concentration has been demonstrated. Flux and selectivity are sensitive functions of ionic strength. These parameters are critical in the use of multilayers as selective media for membrane separations, as well as the loading and release of bioactive molecules from PEMU films and capsules. If multilayer pairs with strong interaction energies are employed, very thin films are required for isolation of charged species. There are several ways to dramatically modify membrane transport rates through reluctant exchangers with a small stimulus: a small change in salt concentration is amplified to a large change in diffusion for multiply charged species. Alternatively, modifying the charge of a species to be transported via a chaperone or carrier can have a dramatic impact on permeation. We have not discussed, for example, those probe ions that, being weak acids/bases, may exist in different charged states. The mobility, and salt dependence, within multilayers is found to depend on the state of probe ion protonation. Details will be presented and analyzed in a forthcoming paper.

(47) Rodriguez, L. N. J.; De Paul, S. M.; Barrett, C. J.; Reven, L.; Spiess, H. W. *Adv. Mater.* **2000**, *12*, 1934.

Also outside the scope of the present report are pH-dependent multilayers.[48] The addition of extrinsic sites within a weak polyacid PEMU via a pH change[8c] is one of several postsynthesis pathways for introducing extrinsic charge ($y_{rpe}$) which, potentially, short circuits the reluctant exchanger resistance to mass transfer. While extrinsic charge can significantly enhance transport, flux control by salt will be degraded (although selectivity may be enhanced). In the limit of significant permanent extrinsic charge of one sign, the system behaves as classical fixed site (Donnan) ion exchanger, permselective to either positive or negative charge.[8h] It should be noted that the tendency for polyelectrolyte ion pairing is strong and any newly created bulk extrinsic charge may well be extruded to the surface, reestablishing bulk intrinsic compensation and reluctant exchanger behavior. Cross-linking may be required to inhibit this internal reorganization of charge.

## Experimental Section

PSS (molecular weight 70 000) and PDADMA ($M_w$ (3−4) × $10^5$), from Aldrich, were dialyzed against distilled water using 3500 molecular weight cutoff dialysis tubing (Spectra/Por). Sodium chloride (Fisher), potassium ferrocyanide (Fisher), hydroquinone (Fisher), sodium perchlorate (Mallinckrodt), ferrous sulfate (Aldrich), and potassium ferricyanide (Mallinckrodt) were used as received.

Electrochemical measurements were performed with a 100-mL cell equipped with a water jacket thermostated to ±0.1 °C, a platinum counter electrode, and a KCl-saturated calomel electrode, against which all potentials are quoted. The working electrode was a platinum rotating disk electrode (RDE, Pine Instruments), 8 mm in diameter, mounted in a Pine ASR2 rotator. Potential ramps were generated by a Princeton Applied Research 273 potentiostat interfaced to a PC.

To prepare the electrode surface for multilayer deposition, it was polished with 0.05-μm alumina (Buehler), sonicated, and rinsed in water. Sequential adsorption of polyelectrolytes onto the RDE at 300 rpm was performed with the aid of a robot (StratoSequence V, nanoStrata Inc.). The two polymer deposition solutions contained 10 mM PSS or 10 mM PDADMA, both in 0.25 M NaCl. Between alternate exposures to the polyelectrolytes, there were three rinses of distilled water. Rinse and polymer solution volumes were ∼50 mL each. The deposition time for each layer was 5 min, and the rinse time 1 min. The last (PSS) layer of 20 was deposited from solution containing 10 mM salt to allow adsorption with minimal surface charge overcompensation.[12]

ATR measurements were performed with a Nicolet Nexus 470 fitted with DTGS detector and a 0.5-mL capacity flow-through ATR assembly (Specac Benchmark) with a 70 × 10 × 6 mm 45° germanium crystal. Each spectrum had 50 scans coadded at a resolution of 4 $cm^{-1}$. Multilayers were deposited on the ATR crystal while it was loaded in the flow cell by passing polyelectrolyte and rinse solutions, in an alternating manner, through the cell. To determine spectrometer response to sulfonate and perchlorate, standard solutions (0.10 M) of PSS and $NaClO_4$ were passed through the cell using a bare crystal. Thicknesses on Pt were determined using a Gaertner Scientific L116B Autogain ellipsometer with 632.8-nm radiation at 70° incident angle. Multilayer thickness on the Ge crystal was measured with a profilometer (Tencor Instruments) at step edges (scratches). All experimental data points have a RSD of ∼±5%.

**Acknowledgment.** The authors are grateful for assistance from Per Rikvold concerning the combinatorics calculations. This research was supported by a grant from the National Science Foundation ((DMR9727717).

**Supporting Information Available:** Extended equilibrium expressions, FTIR spectra, detailed Monte Carlo and probability treatment (PDF). This material is available free of charge via the Internet at http://pubs.acs.org.

JA021448Y

(48) (a) Yoo, D.; Shiratori, S. S.; Rubner, M. F. *Macromolecules* **1998**, *31*, 4309. (b) Mendelsohn, J. D.; Barrett, C. J.; Chan, V. V.; Pal, A. J.; Mayes, A. M.; Rubner, M. F. *Langmuir* **2000**, *16*, 5017.